

Structural and Optical Properties of $Zn_{x-1}Mg_xO$ Ceramic Composites

Zayani Jaafar Othman, Adel Matoussi

Laboratory of Composite Ceramic and Polymer Materials, Scientific Faculty of Sfax, Sfax, Tunisia.
Email: jaafar.zayani@yahoo.fr

Received May 4th, 2012; revised June 5th, 2012; accepted July 6th, 2012

ABSTRACT

In the present work, we investigate the structural and optical properties of $Zn_{x-1}Mg_xO$ composites prepared by the standard sintering method at 1200°C during 24 hours and doped with different percentages of magnesium x between 0% and 40%. For this purpose, we have used the X-ray diffraction (XRD) and the atomic force microscopy (AFM) to study the effect of the magnesium's proportion on the crystalline and morphology proprieties of the obtained samples. XRD analysis showed that all films are polycrystalline with a hexagonal wurtzite structure, with an orientation of the grains according to directions (0002) and (10-10). The AFM characterisation show that the degree of surface roughness (RMS) increases with the increasing of MgO content. Optical properties of the ceramics were investigated by Absorbance and Reflectance measurements at room temperature in the wavelength range 200 - 2400 nm. Optical band gap energies (E_g) were determined. Further cathodoluminescence and dielectric measurements would be carried out to study the influence of MgO doping on the dielectric and luminescent properties of the ZnMgO ceramics.

Keywords: $Zn_{x-1}Mg_xO$ Composites; X-Ray Diffraction; AFM; Optical Properties

1. Introduction

The growth and characterization of II-VI semiconductor ZnO based alloys (including MgZnO, CdZnO, and MnZnO) have been becoming a more and more active research field in recent years. The research interests on ZnO have been encouraged by the industrial and technological demands for the new generation of opto-electronic devices, because of its wide band gap (3.4 eV at 300 K) and large exciton binding energy (60 meV) [1]. ZnO is a promising candidate material for advanced devices applications due to the above-mentioned characteristics and unique combination of its physical properties optical, electrical, magnetic, piezoelectric, and ferroelectric. These characteristics are used in a wide range of applications such as solar cells [2], transparent conducting films, chemical sensors [3,4], varistors [5,6], light-emitting diodes [7], laser diodes [8], etc. Furthermore, ZnO is a reliable candidate operated for high temperature electronic devices that can be surely used in harsh environments [9,10]. ZnO samples have been synthesized by a variety of processes, including vapor deposition [11], pulsed laser deposition [12], molecular beam epitaxy [13], metal organic chemical vapour deposition (MOCVD) [14], sputtering [15], electron beam evaporation [16], spray pyrolysis [17,18], sol-gel processing [19].

In this work, we interested to preparation and charac-

terization of $Zn_{x-1}Mg_xO$ bulk ceramics to study the influence of the MgO content on the structural, morphological and optical properties of the ZnMgO composites for the potential applications in the new optoelectronic devices.

2. Experimental Procedure

$Zn_{x-1}Mg_xO$ composites were prepared by conventional solid state reaction method using a mixture of metallic oxides ZnO and MgO purchased by the GmbH Aldrich Company. The weight content of MgO ($x = 0\% - 40\%$) was added to pure ZnO powder (99.99%) and milled in an agate which calcined at temperature of 500°C for 3 hours in air ambient furnace. The ZnO-MgO powders were pressed into pellets (of 1.5 mm in thickness and 8 mm in diameter) and sintered at a high temperature 1200°C for 24 hrs with heating rate of 10°C/min. Pellets were then cooled slowly to room temperature. X-ray diffraction (XRD) with Cu-K α radiation wavelength of 0.15406 nm was used to determine the crystal structure of ZnMgO ceramics in the scan range $2\theta = 20^\circ - 60^\circ$.

The surface morphology was analysed by Atomic force microscopy (AFM). Optical properties of the ZnMgO pellets were examined in the wavelength range 200 - 1800 nm by using the UV-VIS-NIR spectrophotometer (SHIMADZV UV-3101PC).

3. Results and Discussions

3.1. Structural and Morphological Properties

Figure 1 shows the XRD patterns of $Zn_{x-1}Mg_xO$ pellets for different additive content. All the composites exhibit a polycrystalline hexagonal structure marked by the appearance of peaks corresponding to wurtzite reflections planes (10.0), (00.2), (10.1), (10.2) and (11.0). As the weigh content ($x\%$) is increased, it observed at 36.7° and 42.7° the reflections planes (111) and (200) for cubic phase of MgO. As shown in the inset (**Figure 1**), the intensity of (0002) XRD peak decreases and shifts towards high 2θ angles as the MgO content increases from 0% to 40%. This result suggests that the lattice parameter along the c-axis decreases indicating a compressive strain [20]. The grain sizes, lattice parameters, strains and residual stress values were calculated and presented in the **Table 1**.

The texture coefficient of oriented crystallites was calculated using the well-known formula reported in Ref. [21]. It is found that the highest TC values (greater than 1.2) correspond to (00.2) and (10.1) planes which contribute about oriented grains of 42% and 27% respectively. The average grain sizes of the films are calculated from (0002) diffraction peak using the Scherrer's equation [22]. It can be seen that grain size decreases from 109 nm to 55 nm as x (wt%) varied from 0 to 40. This behaviour is observed in previous works [23,24].

Figure 2 shows the variation of lattice strain and residual stress in $Zn_{x-1}Mg_xO$ ceramic composites with addition of MgO content. It must be noticed that the sample doped with 10% of MgO has larger strain and stress values. The residual stresses σ_{zz} are compressive which tend to decrease from 1016 MPa to 834 MPa when MgO additive content increased from 10% to 40% respectively.

Figure 3 shows AFM images of ZnMgO pellets. The surface morphology is covered by randomly distributed islands with heights in the range $0.3 \mu\text{m} - 1.28 \mu\text{m}$. With increasing MgO content, the surface rms roughness increases from 67.3 nm, 102.45 nm to 252.54 nm as x varied from 0%, 20% and 40% respectively. From the above results, it is seen clearly an improvement of the

microstructure and the crystalline quality of the ZnMgO composite as the doping content increased.

3.2. Optical Properties

In this part, the absorption and reflectance spectra of $Zn_{x-1}Mg_xO$ composites were measured at room temperature using UV-VIS-NIR spectrophotometer. **Figure 4** shows the absorbance of the composites with different MgO contents. The optical transmittance does not measured because the studied pellets are very thicker of about 1.5 mm. In UV wavelength region, the average absorbance decreases approximately from 42% to 22% when MgO content increases from 0% to 30%.

For composition $x = 40\%$, the optical absorbance increased to 51%. One can noticed that all the ZnMgO samples tend to more reflect the visible lights. In the ZnO absorption spectrum, it appears prominent peak at 374.8 nm attributed to the exciton transition, indicating thus a

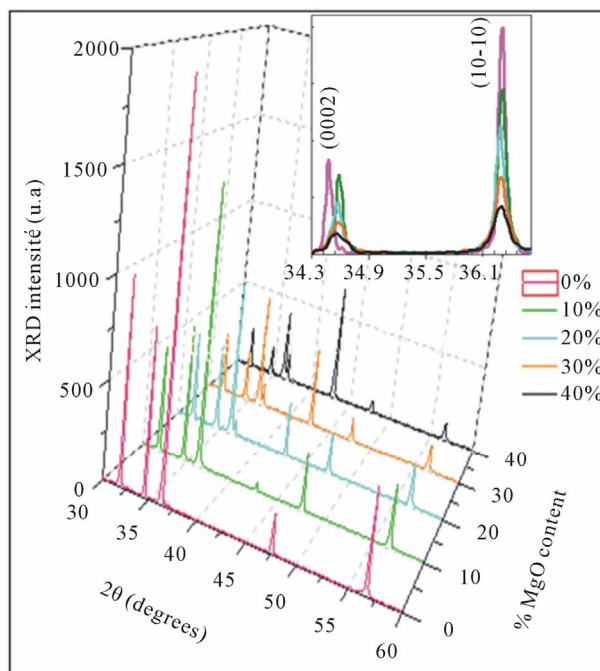


Figure 1. XRD patterns of $Zn_{x-1}Mg_xO$ composite.

Table 1. The grain sizes, texture coefficient (TC), lattice parameters, lattice strain and residual stress values of $Zn_{x-1}Mg_xO$ composites.

MgO (wt%)	a (Å)	c (Å)	TC (00.2)	χ (%) (00.2)	TC (10.0)	χ (%) (10.0)	D (nm)	$E_{zz} (\times 10^{-3})$	Σ_{zz} (GPa)
0	3.247	5.183	2.045	40.9	1.374	27.4	108.94	-1.55	0.355
10	3.249	5.173	2.146	43.3	1.207	24.1	83.43	-4.48	1.016
20	3.252	5.181	1.968	39.3	1.318	26.3	69.88	-4.41	1.002
30	3.251	5.186	2.022	40.4	1.276	25.5	50.49	-4.42	1.003
40	3.250	5.182	2.106	42.1	1.242	24.8	55.72	-3.67	0.834

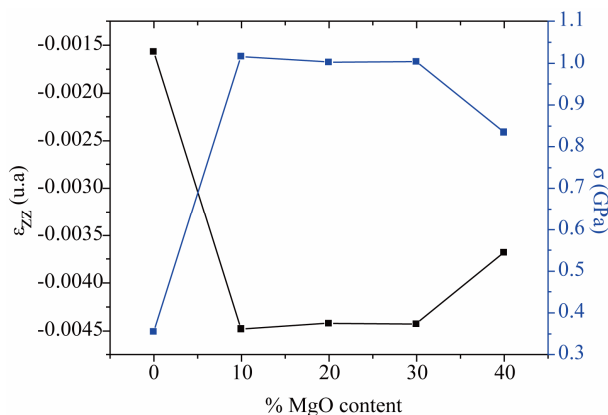


Figure 2. Variation of lattice strain and residual stress in $Zn_{x-1}Mg_xO$ composites with MgO content.

high optical quality of the material.

Figure 5 shows the plots $(\alpha hv)^2$ versus photon energy for all samples. From these curves, we have determined the band gap energy E_g using the following relationship [25]:

$$(\alpha hv) = B(hv - E_g)^{1/2}$$

where B , α , hv are constant, absorption coefficient and energy photon respectively. Determined E_g values are given in the inset (see **Figure 5**).

For MgO composition varied from $x = 0\%$ to 30% , we have observed a decrease in E_g value from 3.42 eV to 3.25 eV respectively. This is consistent with highly doped ZnO samples [26,27]. But, for weight concentration $x = 40\%$, the band gap of MgO-ZnO system reaches a value about 3.71 eV.

This increase can be attributed to the Burstein-Moss effect and/or to the formation of hexagonal ZnMgO alloy phase [28-32]. Chunming Jin [32] and Ohtomo [28] have synthesized single hexagonal $Mg_xZn_{1-x}O$ thin films with x up to 0.36 where its band gap tuned from 3.36 to 4.12 eV. In our case, the observed decrease of E_g can be explained to low solubility of MgO in ZnO [33] and cubic phase MgO segregation as confirmed by XRD analysis. In future, we plan to determine the composition limit ($x_c\%$) above it occurs changes on the structure and optical properties of ZnO-MgO composites. Cathodoluminescence and dielectric measurements would be carried out to study the influence of MgO doping on the dielectric and luminescent properties of the ZnMgO ceramics.

4. Conclusion

$Zn_{x-1}Mg_xO$ composites prepared were deposited by standard sintering method at $1200^\circ C$. The effects of MgO content on the structural, morphological and optical properties of $Zn_{x-1}Mg_xO$ composites were investigated. All the deposited composites are polycrystalline with

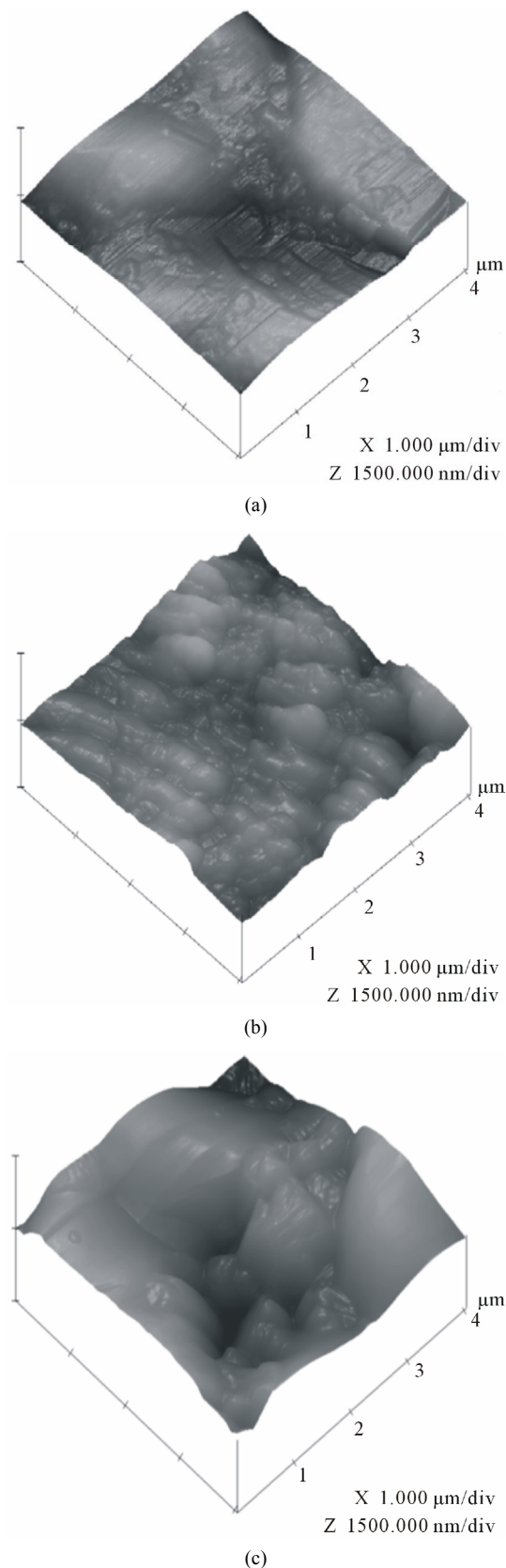


Figure 3. 3D AFM images obtained for $Zn_{x-1}Mg_xO$ composites (a) $x = 0\%$; (b) $x = 20\%$ and (c) $x = 40\%$.

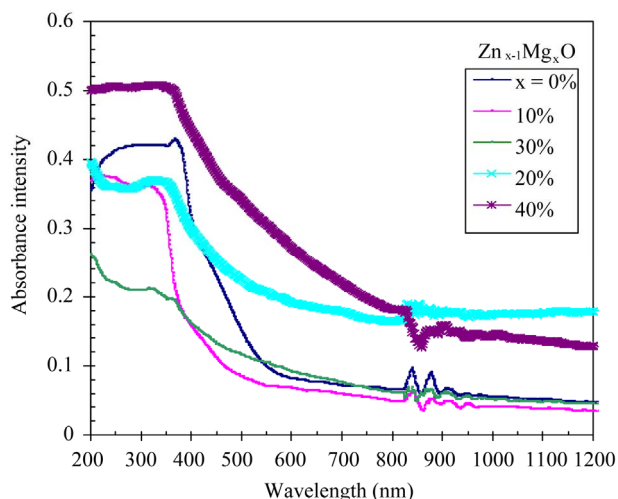


Figure 4. Absorbance spectra of $Zn_{x-1}Mg_xO$ pellets measured at room temperature.

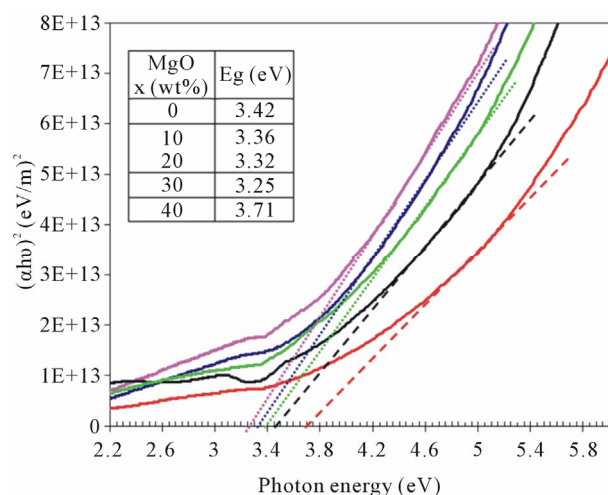


Figure 5. Plots of $(ahv)^2$ vs. photon energy of $Zn_{x-1}Mg_xO$ composites.

hexagonal wurtzite structure. XRD revealed the inclusion of cubic MgO phase as the doping content increased up to 40%. AFM analyses show rms roughness in the range 67.3 - 252.54 nm for $Zn_{x-1}Mg_xO$ ($x = 0 - 0.4$) ceramics. Optical properties of the ceramics were investigated by Absorbance and Reflectance measurements at room temperature in the wavelength range 200 - 2400 nm. We observed decrease in the band gap E_g for concentrations $x \leq 0.3$ and increases when $x = 0.4$. This increase in E_g can be attributed to the formation of ZnMgO alloy structure.

REFERENCES

[1] H. E. Brown, "The Exciton Spectrum of Zinc Oxide," *Journal of Physics and Chemistry of Solids*, Vol. 15, No. 1-2, 1960, pp. 86-89.
 [2] S. Gledhil, A. Grimm, A. Allsop, T. Koehler, C. Camus,

L. Lux-Steiner and C.-H. Fisher, "A Spray Pyrolysis Route to the Undoped ZnO Layer of $Cu(In,Ga)(S,Se)_2$ Solar Cells," *Thin Solid Films*, Vol. 517, No. 7, 2009, pp. 2309-2311.

- [3] S. Major and K. L. Chopra, "Indium-Doped Zinc Oxide Films as Transparent Electrodes for Solar Cells," *Solar Energy Materials*, Vol. 17, No. 5, 1988, pp. 319-327. doi:10.1016/0165-1633(88)90014-7
- [4] S. T. Shishiyanu, T. S. Shishiyanu and O. I. Lupan, "Sensing Characteristics of Tin-Doped ZnO Thin Films as NO_2 Gas Sensor," *Sensors and Actuators B*, Vol. 107, 2005, pp. 379-386. doi:10.1016/j.snb.2004.10.030
- [5] T. K. Gupta, "Applications of Zinc Oxide Varistors," *Journal of the American Ceramic Society*, Vol. 73, No. 7, 1990, pp. 1817-1840. doi:10.1111/j.1151-2916.1990.tb05232.x
- [6] S. Anas, R. V. Mangalaraja, M. Poothayal, S. K. Shukla and S. Ananthakumar, "Direct Synthesis of Varistor-Grade Doped Nanocrystalline ZnO and Its Densification through a Step-Sintering Technique," *Acta Materialia*, Vol. 55, No. 17, 2007, pp. 5792-5801. doi:10.1016/j.actamat.2007.06.047
- [7] Y. I. Alivov, E. V. Kalinina, A. E. Cherenkov, D. C. Look, B. M. Ataev, A. K. Omaev, M. V. Chukichev and D. M. Bagnall, "Fabrication and Characterization of n-ZnO/p-AlGaIn Heterojunction Light-Emitting Diodes on 6H-SiC Substrates," *Applied Physics Letters*, Vol. 83, No. 23, 2003, pp. 4719-4721. doi:10.1063/1.1632537
- [8] H. S. Kim, F. Lugo, S. J. Pearton, D. P. Norton, Y. L. Wang and F. Ren, "Phosphorus Doped ZnO Light Emitting Diodes Fabricated via Pulsed Laser Deposition," *Applied Physics Letters*, Vol. 92, 2008, Article ID: 112108. doi:10.1063/1.2900711
- [9] D. C. Look, D. C. Reynolds, J. W. Hemsky, R. L. Jones and J. R. Sizelove, "Production and Annealing of Electron Irradiation Damage in ZnO," *Applied Physics Letters*, Vol. 75, No. 6, 1999, pp. 811-813. doi:10.1063/1.124521
- [10] C. Coskun, D. C. Look, G. C. Farlow and J. R. Sizelove, "Radiation Hardness of ZnO at Low Temperatures," *Semiconductor Science and Technology*, Vol. 19, No. 6, 2004, pp. 752-754. doi:10.1088/0268-1242/19/6/016
- [11] Y. I. Alivov, J. E. Van Nostrand and D. C. Look, "Observation of 430 nm Electroluminescence from ZnO/GaN Heterojunction Light-Emitting Diodes," *Applied Physics Letters*, Vol. 83, No. 14, 2003, pp. 2943-2945. doi:10.1063/1.1615308
- [12] R. Perez-Casero, A. Gutierrez-Llorente, O. Pons-y-Moll, W. Seiler, R. M. Defourneau, D. Defourneau, E. Millon, J. Perriere, P. Goldner and B. Viana, "Er-Doped ZnO Thin Films Grown by Pulsed-Laser Deposition," *Applied Physics Letters*, Vol. 97, No. 5, 2005, Article ID: 054905.
- [13] D. C. Oh, T. Suzuki, J. J. Kim, H. Makino, T. Hanada, M. W. Cho and T. Yao, "Electron-Trap Centers in ZnO Layers Grown by Molecular-Beam Epitaxy," *Applied Physics Letters*, Vol. 86, No. 3, 2005, Article ID: 032909. doi:10.1063/1.1849852
- [14] W. Z. Xu, Z. Z. Ye, Y. J. Zeng, L. P. Zhu, B. H. Zhao, L. Jiang, J. G. Lu, H. P. He and S. B. Zhang, "ZnO

- Light-Emitting Diode Grown by Plasma-Assisted Metal Organic Chemical Vapor Deposition,” *Applied Physics Letters*, Vol. 88, No. 17, 2006, Article ID: 173506. doi:10.1063/1.2199588
- [15] D.-K. Hwang, S.-H. Kang, J.-H. Lim, E.-J. Yang, J.-Y. Oh, J.-H. Yang and S.-J. Park, “*p*-ZnO/*n*-GaN Heterostructure ZnO Light-Emitting Diodes,” *Applied Physics Letters*, Vol. 86, No. 22, 2005, Article ID: 222101. doi:10.1063/1.1940736
- [16] A. Kuroyanagi, “Properties of Aluminum-Doped ZnO Thin Films Grown by Electron Beam Evaporation,” *Japanese Journal of Applied Physics*, Vol. 28, 1989, pp. 219-222. doi:10.1143/JJAP.28.219
- [17] J. De Merchant and M. Cocivera, “Preparation and Doping of Zinc Oxide Using Spray Pyrolysis,” *Materials Chemistry*, Vol. 7, No. 9, 1995, pp. 1742-1749.
- [18] P. Nunes, B. Fernandes, E. Fortunato, P. Vilarinho and R. Martins, “Performances Presented by Zinc Oxide Thin Films Deposited by Spray Pyrolysis,” *Thin Solid Films*, Vol. 337, No. 1-2, 1999, pp. 176-179. doi:10.1016/S0040-6090(98)01394-7
- [19] Z. B. Shao, C. Y. Wang, S. D. Geng, X. D. Sun and S. J. Geng, “Fabrication of Nanometer-Sized Zinc Oxide at Low Decomposing Temperature,” *Journal of Materials Processing Technology*, Vol. 178, No. 1-3, 2006, pp. 247-250. doi:10.1016/j.jmatprotec.2006.03.174
- [20] M. Chaari, A. Matoussi and Z. Fakhfakh, “Structural and Dielectric Properties of Sintering Zinc Oxide Bulk Ceramic,” *Materials Sciences and Application*, Vol. 2, No. 7, 2011, pp. 764-769. doi:10.4236/msa.2011.27105
- [21] Y. Caglar, S. Aksoy, S. Ilican and M. Cagmar, “Crystal-line Structure and Morphological Properties of Undoped and Sn Doped ZnO Thin Films,” *Superlattices and Microstructures*, Vol. 46, 2009, pp. 469-475. doi:10.1016/j.spmi.2009.05.005
- [22] B. D. Cullity and S. R. Stock, “Elements of X-Ray Diffraction,” 3rd Edition, Prentice Hall, Upper Saddle River, 2001.
- [23] P. M. Ratheesh Kumar, C. Sudha Kartha, K. P. Vijayakumar, F. Singh and D. K. Avasthi, “Effect of Fluorine Doping on Structural, Electrical and Optical Properties of ZnO Thin Films,” *Materials Science and Engineering: B*, Vol. 117, No. 3, 2005, pp. 307-312. doi:10.1016/j.mseb.2004.12.040
- [24] A. Sanchez-Juarez, A. Tiburcio-Silver and A. Ortiz, “Properties of Fluorine-Doped ZnO Deposited onto Glass by Spray Pyrolysis,” *Solar Energy Materials and Solar Cells*, Vol. 52, No. 3-4, 1998, pp. 301-311. doi:10.1016/S0927-0248(97)00246-8
- [25] J. I. Pankove, “Optical Processes in Semiconductors,” Prentice-Hall Inc., Upper Saddle River, 1971.
- [26] S. Ilican, Y. Caglar, M. Caglar and B. Demirci, “Polycrystalline Indium-Doped ZnO Thin Films: Preparation and Characterization,” *Journal of Optoelectronics and Advanced Materials*, Vol. 10, No. 10, 2008, pp. 2592-2598.
- [27] H. Abdelkader, Y. Fayssal, D. Warda, A. Nadhir and A. M. Salah, “Les Propriétés Structurales, Optiques et Électriques des Couches Minces de ZnO:Al Élaborées par Spray Ultrasonique,” *Nature and Technologie*, No. 6, 2011, pp. 25-27.
- [28] A. Ohtomo, *et al.*, “ $Mg_xZn_{1-x}O$ as a II-VI Widegap Semiconductor Alloy,” *Applied Physics Letters*, Vol. 72, No. 19, 1998, pp. 2466-2468. doi:10.1063/1.121384
- [29] A. K. Sharma, J. Narayan, J. F. Muth, C. W. Teng, C. Jin, A. Kvit, R. M. Kolbas and O. W. Holland, “Optical and Structural Properties of Epitaxial $Mg_xZn_{1-x}O$ Alloys,” *Applied Physics Letters*, Vol. 75, No. 21, 1999, pp. 3327-3329. doi:10.1063/1.125340
- [30] Z. K. Tang, G. K. L. Wong, P. Yu, M. Kawasaki, A. Ohtomo, H. Koiyama and Y. Segawa, “Room-Temperature Ultraviolet Laser Emission from Self-Assembled ZnO Microcrystallite Thin Films,” *Applied Physics Letters*, Vol. 72, No. 25, 1998, pp. 3270-3272. doi:10.1063/1.121620
- [31] H. Cao, Y. G. Zhao, H. C. Ong, S. T. Ho, J. Y. Wu and R. P. H. Chang, “Ultraviolet Lasing in Resonators Formed by Scattering in Semiconductor Polycrystalline Films,” *Applied Physics Letters*, Vol. 73, No. 25, 1998, pp. 3656-3658. doi:10.1063/1.122853
- [32] C. Jin and R. J. Narayan, “Structural and Optical Properties of Hexagonal $Mg_xZn_{1-x}O$ Thin Films,” *Journal of Electronic Materials*, Vol. 35, No. 5, 2006, pp. 869-876. doi:10.1007/BF02692542
- [33] E. R. Segnit and A. E. Holland, “The System MgO-ZnO-SiO₂,” *Journal of the American Ceramic Society*, Vol. 48, No. 8, 1965, pp. 409-413. doi:10.1111/j.1151-2916.1965.tb14778.x